RNA Silencing of Checkpoint Regulators Sensitizes *p53*-Defective Prostate Cancer Cells to Chemotherapy while Sparing Normal Cells

Utpal K. Mukhopadhyay,[1] Adrian M. Senderowicz,[2] and Gerardo Ferbeyre[1]

[1]Département de Biochimie, Université de Montréal, Montreal, Quebec, Canada and [2]Oral and Pharyngeal Cancer Branch, National Institute of Dental and Craniofacial Research, NIH, Bethesda, Maryland

Abstract

***p53* is frequently mutated in patients with prostate cancer, especially in those with advanced disease. Therefore, the selective elimination of *p53* mutant cells will likely have an impact in the treatment of prostate cancer. Because *p53* has important roles in cell cycle checkpoints, it has been anticipated that modulation of checkpoint pathways should sensitize *p53*-defective cells to chemotherapy while sparing normal cells. To test this idea, we knocked down ataxia telangiectasia mutated (*ATM*) gene by RNA interference in prostate cancer cell lines and in normal human diploid fibroblasts IMR90. *ATM* knockdown in *p53*-defective PC3 prostate cancer cells accelerated their cell cycle transition, increased both E2F activity and proliferating cell nuclear antigen expression, and compromised cell cycle checkpoints, which are normally induced by DNA damage. Consequently, PC3 cells were sensitized to the killing effects of the DNA-damaging drug doxorubicin. Combining *ATM* knockdown with the Chk1 inhibitor UCN-01 further increased doxorubicin sensitivity in these cells. In contrast, the same strategy did not sensitize either IMR90 or LNCaP prostate cancer cells, both of which have normal *p53*. However, IMR90 and LNCaP cells became more sensitive to doxorubicin or doxorubicin plus UCN-01 when both *p53* and *ATM* functions were suppressed. In addition, knockdown of the G_2 checkpoint regulators *ATR* and *Chk1* also sensitized PC3 cells to doxorubicin and increased the expression of the E2F target gene *PCNA*. Together, our data support the concept of selective elimination of *p53* mutant cells by combining DNA damage with checkpoint inhibitors and suggest a novel mechanistic insight into how such treatment may selectively kill tumor cells.** (Cancer Res 2005; 65(7): 2872-81)

Introduction

Cell cycle checkpoints are signaling pathways that sense the state of the cell and the progression of cell cycle events to orchestrate a cellular response to damage (1). The outcome of activating checkpoints depends on the extent of the damage. Moderate injury generally triggers a cell cycle arrest to allow time for repair, dissipation of stressors, or accumulation of essential factors for cell cycle progression. On the other hand, significant damage induces programmed cell death to protect the organism from the expansion of cells with extensive genomic alterations that could eventually lead to neoplastic transformation (2). Failure to activate these checkpoint pathways may cause the development of cancer and other diseases (2). In agreement, cancer cells have altered checkpoint mechanisms that help them to maintain cell proliferation in the presence of oncogenic stress. Therefore, a major issue in cancer therapeutics is to find targets whose modulation will exploit these checkpoint defects in tumor cells to make them more sensitive to chemotherapy (3).

One of the most common genetic alterations in cancer patients involves the *p53* tumor suppressor gene. In prostate cancer, altered *p53* expression has been correlated with a higher Gleason score and worse prognosis (4–9). *p53* mutations occur early in the process of prostate tumorigenesis inasmuch as they have been found in prostatic intraepithelial neoplasia and benign prostatic hyperplasia (10–14). Significantly, cells with *p53* mutations found in primary prostate tumors seemed clonally expanded in their metastases (15, 16). Collectively, these studies indicate that the *p53* tumor suppressor pathway is often disrupted in prostate neoplasms.

As a rule, cells with defective *p53* fail to undergo apoptosis in response to a variety of proapoptotic stimuli and generally have a growth advantage over cells that have intact *p53* (17). However, *p53* is also involved in DNA repair and is an important component of cell cycle checkpoints. Consequently, *p53* null cells have increased sensitivity to certain DNA-damaging stress (18, 19). For instance, caffeine, which inhibits the G_2 checkpoint, sensitizes *p53* null cells to radiation (20, 21). One of the most important mediators of the checkpoint pathways is the caffeine target ataxia telangiectasia mutated (*ATM*). ATM is a member of the phosphatidylinositol 3-kinase family of proteins that also includes ATM and ATR, DNA-PK, and mTor. ATM activates DNA repair and checkpoint pathways by phosphorylating multiple targets, including p53, Mdm2, BRCA1, Chk2, and Nbs1 (22). It has been shown that an antisense RNA directed against *ATM* renders prostate cancer cells more sensitive to radiation (23, 24), suggesting that disabling ATM might be part of an approach aimed to kill tumor cells.

Recently, Collis and colleagues used RNA interference (RNAi) to knock down *ATM*, *DNA-PK*, or *ATR* in prostate cancer cell lines. Knocking down ATM or DNA-PK sensitized the cells to radiation whereas the small interfering RNA against ATR sensitized the cells to the DNA-damaging agent methyl methanesulfonate (25). This study was done with *p53*-disabled prostate cancer cell lines that are also known for containing other genetic changes. Therefore, it was not possible to conclude that the *p53* status determined the chemosensitizing effect of knocking down checkpoint proteins. In addition, the effects of silencing checkpoint regulators in normal cells were not investigated. This is relevant, because in theory modulation of checkpoints would be more effective in cells deficient for *p53* (3, 18, 19, 26).

To address these issues we developed a retroviral vector system for stable expression of small hairpin RNAs (shRNA) in prostate cancer cells and normal human diploid fibroblasts. We achieved a

Note: Supplementary data for this article are available at Cancer Research Online (http://cancerres.aacrjournals.org/).

Requests for reprints: Gerardo Ferbeyre, Département de Biochimie, Université de Montréal, E-515 C.P. 6128, Succursale Centre-Ville, Montreal, Quebec, Canada H3C 3J7. Phone: 514-343-7571; Fax: 514-343-2210; E-mail: g.ferbeyre@umontreal.ca.

stable and almost complete inhibition of ATM, ATR, and Chk1 levels in the *p53* null PC3 prostate cancer cells, rendering them more sensitive to doxorubicin. Treatment with the G_2 checkpoint inhibitor UCN-01 cooperated with the anti-*ATM* shRNA to promote drug sensitivity. We also found that *ATM* knockdown increased the mitotic index of PC3 prostate cancer cells, augmented E2F activity and proliferating cell nuclear antigen (*PCNA*) expression, and inhibited G_2 arrest in response to DNA damage. Significantly, RNAi against *ATM* did not increase the chemosensitivity of *p53*-proficient normal fibroblasts or the prostate cancer cell line LNCaP. However, upon *p53* inhibition, those cells became sensitized to doxorubicin by the anti-*ATM* shRNA as observed in the *p53* mutant PC3 cells. Finally, we discuss a new model proposing that chemosensitivity after *ATM* knockdown in *p53* mutant cells possibly results from the combined effect of checkpoint defects, low levels of p21, high E2F activity, and increased *PCNA* expression.

Materials and Methods

Cell lines and culturing. Prostate cancer cell lines PC3 (American Type Culture Collection, Manassas, VA) and LNCaP and their derivatives were grown in RPMI (Invitrogen, San Diego, CA). Human diploid fibroblast cells IMR90, their derivatives, and packaging cells Bing and Phoenix were grown in DMEM (Invitrogen). Both media were supplemented with 10% fetal bovine serum (Life Technologies, Inc., Gaithersburg, MD), 2 mmol/L L-glutamine (Life Technologies), and 1% streptomycin-penicillin sulfate (Life Technologies). All cell lines were grown in 5% CO_2 at 37°C in an incubator.

Transfection of PC3 and LNCaP cells were carried out using Metafectene (Biontex, Munich, Germany) according to manufacturer instructions. For monitoring transfection, an enhanced green fluorescent protein (EGFP) expression plasmid (pLPC-GFP) was cotransfected with shRNA-expressing PCR cassettes.

Retroviral infections were done as described (27). However, to increase infection efficiency in PC3 cells, retroviruses were pseudotyped with VSV-G by cotransfecting a VSV-G-expressing plasmid with the retroviral plasmid into the packaging cell line.

Infected PC3 and IMR90-derived cell lines were selected with 2 μg/mL of puromycin (Sigma, St. Louis, MO). Infected LNCaP-derived cell lines were selected with 5 μg/mL of puromycin for 2 days wherever applicable. IMR90 and LNCaP expressing dominant-negative *p53* were grown in the presence of 50 (IMR90) or 100 μg/mL hygromycin (LNCaP).

Construction of retroviral vectors expressing anti-*ATM* small hairpin RNAs and hammerhead ribozymes. Plasmid pMSCV-puro was obtained from Clontech (Palo Alto, CA). pLPC-GFP and pWZL dominant-negative *p53* were described in refs. (27, 28). Two shRNAs, each against human *ATM*, *ATR*, and *Chk1* sequences (GenBank accession nos. NM-000051, NM-001184, and AF016582, respectively), were designed with the "RNAi oligo retriever" software (http://www.cshl.org/public/SCIENCE/hannon.html). The corresponding nucleotide positions targeted (with respect to "A" of AUG as +1) were 1-29 and 9062-9091 for *ATM*; 1-29 and 70-98 for *ATR*, and 48-76 and 92-112 for *Chk1*. The short hairpin activated gene silencing–PCR technique (29) was used to synthesize an expression cassette containing U6 promoter, target-specific hairpin sequence, and *Pol*III terminator using pGEMU6 (N. Hernandez, Cold Spring Harbor Laboratory, Cold Spring Harbor, NY) as template. Two restriction endonuclease sites (*Bgl*II and *Eco*RI) were also incorporated through primers for convenient directional cloning (Supplementary Fig. 1*A*). Resulting 600-bp PCR products were either cloned between *Bgl*II and *Eco*RI sites of retroviral vector pMSCV-puro (Clontech) or used directly for transfection. To control the shRNA experiments we used a retroviral vector expressing a hairpin that does not recognize any human protein (control hairpin). Ribozyme constructs are described in Supplementary Fig. 1*B*.

Fluorescence-activated cell sorting and cell cycle analysis. Cells were cotransfected with equimolar quantities of pLPC-GFP plasmid along with shRNA/hammerhead ribozyme expression cassette. Twelve to 24 hours post transfection, cells were trypsinized, washed with PBS, and resuspended in PBS at a concentration of 2×10^6 cells/mL. EGFP+ cells were sorted using FACS Vantage SE (Becton Dickinson, San Jose, CA) flow cytometer with a laser excitation wavelength of 488 nm and a band-pass filter at 530 ± 30 nm. Data were analyzed by the software CellQuest (version 3.3).

For cell cycle analysis, 3×10^5 cells were plated onto 6-cm plates and grown overnight. Doxorubicin (20 ng/mL) was added 24 hours after plating and 12 hours before harvesting. UCN-01 treatment was started 30 minutes before the addition of doxorubicin. Trypsinized cells were washed and resuspended in PBS. Then they were fixed with an equal volume of ethanol, washed twice with PBS, and treated with RNase (100 μg/mL in 1.12% sodium citrate) for 60 minutes at 37°C. Finally, DNA was stained with the addition of 100 μL of 50 μg/mL propidium iodide solution in 1.12% sodium citrate for 60 minutes at room temperature. Propidium iodide–stained cells were analyzed using FACS Calibur (Becton Dickinson) flow cytometer with a band-pass filter at 585 ± 42 nm. Data were analyzed by ModFit (version 3.1) software.

Analysis of mitotic index. Two sets of 2.5×10^5 cells per condition were plated onto 6-cm plates. To one set, we added 100 ng/mL nocodazole (Sigma) 14 hours after plating. To the other set, along with nocodazole, we also added 100 ng/mL doxorubicin. Cells were harvested 2, 4, and 6 hours post treatment. Subsequent steps of fixation, permeabilization, and staining with Alexa Fluor conjugated phosphohistone H3 (Ser^{10}) antibody (Cell Signalling Technology, Beverly, MA), were carried out per manufacturer's instructions. Antibody-stained cells were analyzed using FACS Calibur (Becton Dickinson) flow cytometer. For each sample, 10,000 cells were analyzed with an excitation wavelength of 633 nm (red diode) and emission at 660 nm (FL4). Data acquisition and analysis were carried out by CellQuest (version 3.3) software.

Cell death and DNA ladder assay. For the cell death assay, we plated 2×10^4 cells per well in 12-well plates in triplicate. Drugs (20 ng/mL of doxorubicin and 100 nmol/L UCN-01) were added 12 hours after plating and the cells were grown for 4 days. At the end of incubation, both attached and floating cells were harvested by trypsinization and centrifugation. The resulting cell pellet was resuspended in PBS plus an equal volume of 0.4% trypan blue staining solution and allowed to stand at room temperature for 30 minutes. Stained and nonstained cells were counted under light microscope. To characterize apoptosis, cells were incubated for 2 days in the absence or presence of drugs (100 ng/mL of doxorubicin and 100 nmol/L UCN-01). DNA fragmentation was detected as described (30).

Cell growth assay. Growth of *p53*-proficient/deficient human fibroblast cell lines IMR90/IMR90dnp53 derivatives was monitored by crystal violet dye retention assay (31). A total of 2×10^4 cells per well in triplicate were plated onto 12-well plates. Twelve hours after plating, one set of plates was fixed with 0.5% glutaraldehyde and stored at +4°C to be used as 0-day control, whereas the other set was allowed to grow for further 6 days and then fixed as before. Fixed cells were stained with 0.5% crystal violet and extensively washed with water. The retained dye was extracted in 0.5 to 2 mL of 10% (v/v) acetic acid solution. An aliquot (0.1-0.2 mL) was placed into a 96-well plate and absorbance was read at 595 nm in a microplate reader.

Clonogenic cell survival assay. Five hundred cells per well were plated onto 6-well plates. Colonies appeared ~8 to 12 days after plating. They were fixed with 0.5% glutaraldehyde, stained with 0.5% crystal violet, and counted. Data are displayed as mean ± SD of at least three independent experiments.

Western blotting. Whole-cell lysates equivalent to 25 to 100 μg total protein were resolved through 6% to 10% SDS-PAGE. Resolved proteins were transferred onto polyvinylidene difluoride membranes and probed with specific antibodies. The following antibodies were used: anti-ATM (from M.B. Kastan, St. Jude Children's Research Hospital, TN) anti-p21 (C-19, 1:250, Santa Cruz Biotechnology, Santa Cruz, CA), anti-PCNA (PC10, 1:2000, from B. Stillman, Cold Spring Harbor, NY), anti-phospho-Thr^{68} Chk2 (2661, 1:1000, Cell Signaling), anti-tubulin (B-5-1-2, 1:5000, Sigma), anti-ATR (N-19, 1:500, Santa Cruz Biotechnology), and anti-Chk1 (FL-476, 1:500, Santa Cruz Biotechnology). The proteins were visualized using respective species-specific, horseradish peroxidase–conjugated secondary antibodies (Sigma) and Lumilight Plus (Amersham, Uppsala, Sweden) chemiluminesence detection kit.

E2F luciferase reporter assay. E2F activity was measured using the Dual-Luciferase Reporter 1000 Assay System (Promega, Madison, WI) according to the manufacturer's instructions. We used the plasmid HsOrc1-luc as E2F reporter (32) and the *Renilla* luciferase pRL plasmid as internal control.

Results

Hammerhead ribozymes and small hairpin RNAs against *ATM* provide reagents for a graded inhibition of *ATM* gene expression. To inhibit the expression of *ATM*, we designed two RNA hairpins with complementarity to sequences in the NH_2- and COOH-terminal ends of the protein coding sequence. We also designed two hammerhead ribozymes targeted against approximately the same regions of the mRNA. We included polyadenylic acid sequences in the 3′ end of the ribozyme to increase their activity (33). shRNA expression cassettes (Supplementary Fig. 1*A*) and ribozymes encoding sequences (Supplementary Fig. 1*B*), were subcloned into the pMSCV retroviral vector and stably introduced into PC3 prostate cancer cells by retroviral infections. Hairpins were more efficient than ribozymes in inhibiting *ATM* expression. ATM-Hp2 was the most efficient, followed by ATM-Hp1 and then Rz1. Rz2 showed no effect (Fig. 1*A*). These gene knockdown effects were sustained for at least 10 passages after retroviral infection (Fig. 1*A*). Neither the hairpins nor the ribozymes reduced PC3 cells growth or their clonogenic ability (not shown). The ability of the most efficient shRNA to interfere with the *ATM* pathway was also verified by measuring the phosphorylation of the ATM target Chk2 at Thr^{68} (Fig. 1*B*). Both basal and drug-induced phosphorylation of Chk2 were significantly inhibited by expression of the anti–ATM-Hp2.

Chemosensitivity in PC3 cells expressing anti-*ATM* small hairpin RNAs or anti-*ATM* ribozymes. To study whether expression of RNA hairpins and ribozymes enhance the sensitivity of PC3 prostate cancer cells to the DNA-damaging drug doxorubicin, we generated stable cell populations expressing the two hairpins and the two ribozymes described above. We treated these cell populations with doxorubicin or a combination of doxorubicin and UCN-01. The latter is known for inhibiting the G_2 checkpoint regulator Chk1 (34). The concentration of doxorubicin used (20 ng/mL) was selected after pilot experiments to determine the maximum amount of drug that revealed survival differences between PC3 and its derivatives expressing anti-*ATM* shRNAs. The concentration of UCN-01 (100 nmol/L) did not significantly affect the viability of PC3 (Supplementary Fig. 1*C*). We found that both anti-*ATM* shRNAs and Rz1 sensitized the cells to doxorubicin (Fig. 1*C*). The degree of sensitization was dependent on the degree of inhibition of *ATM* expression (Fig. 1*A* and *C*). Of note, the combination of doxorubicin and the Chk1 inhibitor UCN-01 promoted an even more potent clonogenic cell death (Fig. 1*C*). Retrovirally derived ATM-Hp2 increased drug sensitivity by a factor of 3.1 and ATM-Hp1 by a factor of 1.9 (Fig. 1*D*). Increased sensitivity to doxorubicin was seen in a dose response experiment as well, wherein anti-ATM-Hp2 reduced both the IC_{50} and the IC_{90} for the drug (Fig. 1*E*). Furthermore, the time required for complete clonogenic cell death after treatment with a combination of doxorubicin (40 ng/mL) and UCN-01 (100 nmol/L) was reduced upon expression of ATM-Hp2. Four days were sufficient to attain 100% killing in cells expressing ATM-Hp2, whereas a significant fraction of cells with a vector control survived even 5 days of treatment (Supplementary Fig. 1*D*).

Next we evaluated the ability of shRNAs and ribozymes to enhance chemosensitivity in transient transfection assays. To this end, cells were cotransfected with EGFP-expressing vector and EGFP-positive cells were sorted by fluorescence-activated cell sorting and treated with doxorubicin or a combination of doxorubicin and UCN-01. The results are presented in Supplementary Fig. 2. Chemosensitivity was enhanced by a factor of 1.8 for ATM-Hp2, 1.4 for ATM-Hp1, and very slightly for ATM-Rz1. Therefore, although the efficiency of killing was higher when the anti-*ATM* hairpins were stably expressed it was also possible to sensitize PC3 cells to doxorubicin in transient assays.

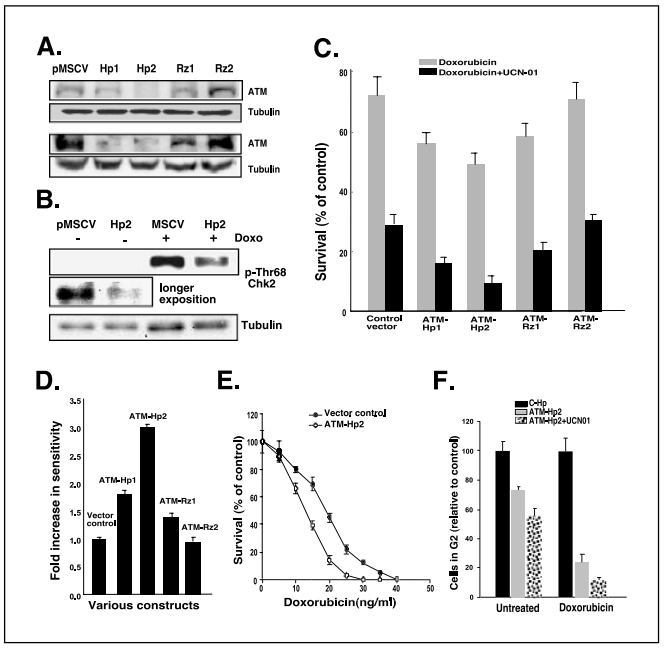

Figure 1. Chemosensitization of PC3 prostate cancer cells by shRNAs and ribozymes against *ATM* and UCN-01. *A,* immunoblots of ATM in PC3 stably transduced with retroviral vector constructs expressing anti-*ATM* shRNAs (*Hp*) or hammerhead ribozymes (*Rz*). Samples were taken 2 (*top*) and 10 (*bottom*) passages after introduction of shRNAs. *Doxo,* doxurubicin. *B,* phospho-Thr^{68} Chk2 in PC3 cells expressing a vector control or anti-ATM-Hp2. *C,* clonogenic assay of PC3 cells stably transduced with various retroviral constructs and treated with doxorubicin or doxorubicin + UCN-01. For each transduced cell line, the viability of untreated cells is taken as 100% and is not shown in the graph for clarity. *D,* fold increase in sensitivity to drug combination (i.e., doxorubicin + UCN-01) for *ATM*-suppressed PC-3 cells were calculated from the results presented in *C* by dividing the percent survival in respective vector control with percent survival in cells stably transduced with various anti-*ATM* constructs. *E,* clonogenic survival of ATM-Hp2 or control vector transduced PC3 cells treated with combination of 100 nmol/L UCN-01 and different concentrations of doxorubicin as indicated. *F,* effect of shRNA against *ATM*, and a control shRNA on the relative number of cells in the G_2-M stage of the cell cycle in cells treated or not treated with doxorubicin or UCN-01. *Points* and *columns,* average of three means; *bars,* SD.

It has been proposed that inhibiting *ATM* expression in *p53* null cells increases drug sensitivity because *p53* mutant cells use G_2 checkpoint pathways controlled by *ATM* in response to DNA damage (20, 23, 24). Consistent with that proposal we observed a reduction in the number of cells in G_2 after *ATM* knockdown by RNAi in PC3 cells (Fig. 1*F*). This reduction was further increased by UCN-01 and was more notorious after treatment with low doses of doxorubicin (Fig. 1*F*). Notably, this decrease in G_2 cells was not accompanied by a preferential accumulation of cells into G_1 or S phases (not shown) suggesting that *ATM*-disabled PC3 cells were not activating checkpoints in G_1 and S. This result is consistent with the *p53* status of PC3 cells.

Effects of *ATM* knockdown on the cell cycle and the G_2 checkpoint in PC3 cells. Next, we wanted to confirm that *ATM* knockdown in *p53*-deficient cells impaired the G_2 checkpoint, increasing cell cycle progression into mitosis. To this end, cells

were treated with doxorubicin to induce DNA damage and nocodazol to stop the cell cycle at mitosis. Mitotic cells were detected using an anti-phosphohistone H3 (Ser^{10}) antibody (Fig. 2*A*). As expected, the number of cells entering mitosis in PC3 cells bearing a vector control was reduced after treatment with doxorubicin. *ATM* knockdown in PC3 cells also reduced the number of cells getting into mitosis, perhaps a reflection of the activation of compensatory G_2 checkpoint proteins such as ATR. However, in contrast to PC3 cells bearing the vector control, a larger fraction of *ATM*-disabled cells still entered mitosis in the presence of doxorubicin (Fig. 2*A*). Even more remarkable, *ATM*-disabled cells displayed an increase in mitotic cells (mitotic index) in the absence of drug, suggesting that ATM slows down the cell cycle in the absence of DNA-damaging drugs as well. In agreement with this idea, *ATM* knockdown was accompanied by a dramatic increase in PCNA (Fig. 2*B*), a protein associated with high proliferation rates and DNA synthesis (35). *PCNA* and many other genes involved in DNA replication are regulated by the E2F family of transcription factors (36). Because E2F1 has been associated with drug response and drug sensitivity in *p53*-defective cells (37, 38), we evaluated total E2F activity in PC3 cells expressing a vector control or anti–ATM-Hp2. To do this, we did reporter assays using a well-known E2F-responsive promoter (32). We found that ATM-Hp2 increased E2F activity in PC3 cells (Fig. 2*C*) and this effect was even more pronounced after treatment with doxorubicin. Hence, suppressing *ATM* gene expression in PC3 cells accelerated cell cycle progression, increased E2F activity and *PCNA* expression, and impaired the G_2 checkpoint. Consequently, these cells entered mitosis in the presence of DNA-damaging drugs.

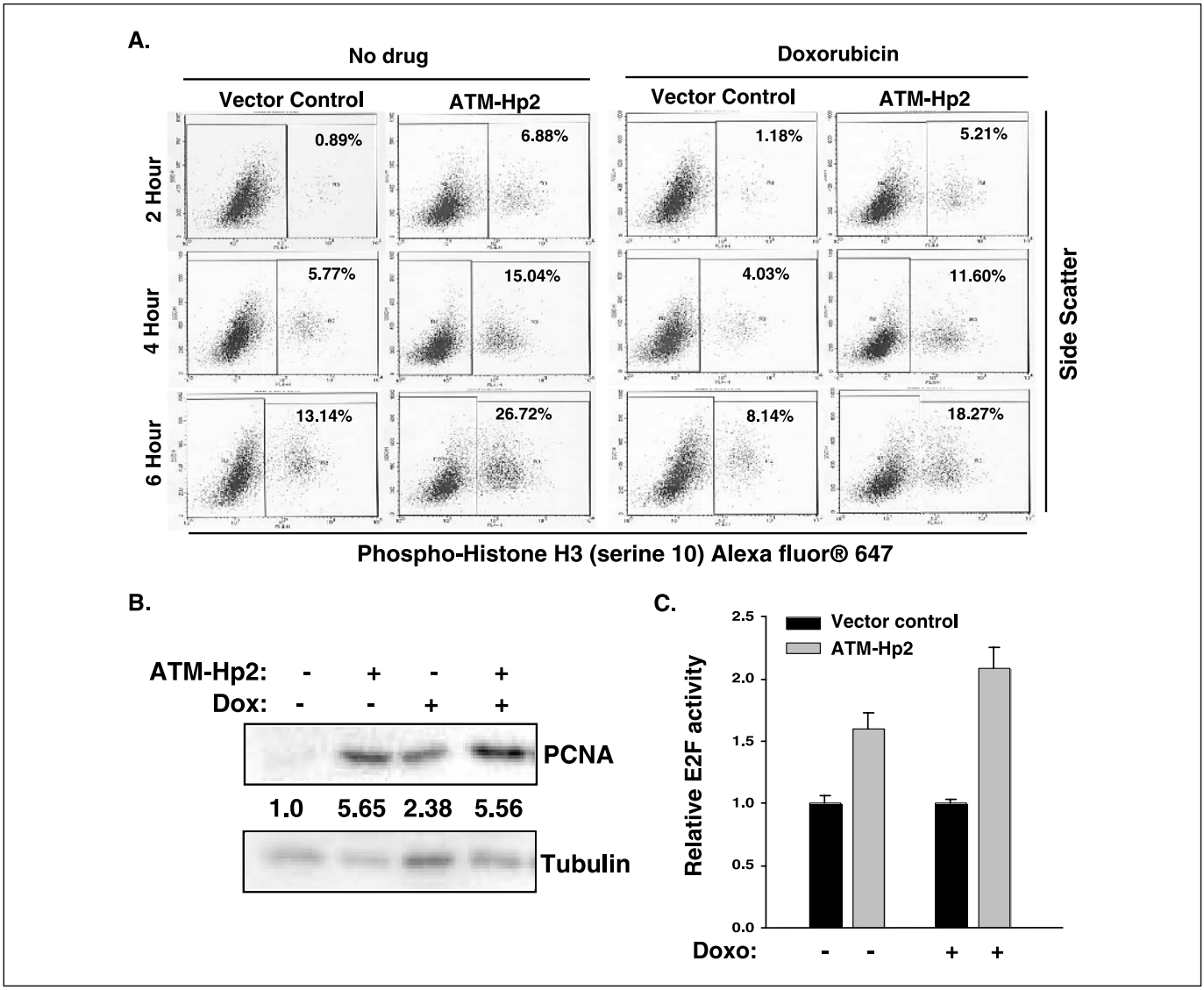

Figure 2. Effect of *ATM* knockdown on mitotic index, *PCNA* expression, and E2F activity in PC3 cells. *A,* percent of mitotic cells labeled with Alexa-conjugated anti-phosphohistone H3 (Ser^{10}) antibody in PC3 cells with *Vector Control* or anti-*ATM* shRNA (*ATM-Hp2*). *Left,* no drug; *right,* 100 ng/mL doxorubicin. *B, PCNA* expression in PC3 cells expressing a vector control or anti–ATM-Hp2. The intensity of the bands was quantified by densitometry. Levels were normalized to tubulin and expressed relative to the value of the *top lane*. *C, ATM* knockdown increases E2F activity. PC3 cells cotransfected with the luciferase reporter construct HsOrc1-luc, which contains E2F sites, and a vector control or its derivative expressing anti–ATM-Hp2. Cells were then treated with doxorubicin or vehicle. *Columns,* mean of three independent measurements; *bars,* SD.

Inhibition of Chk1 and ATR also increased *PCNA* expression in PC3 cells. Next, we wanted to investigate the effects of inhibiting the ATR/Chk1 checkpoint pathway in *p53*-deficient PC3 cells. To do the experiments we first tested several shRNAs against *ATR* and *Chk1* and found one for each gene that efficiently suppressed their expression (Fig. 3*A*). Knocking down either *ATR* or *Chk1* after transient transfection of PC3 cells with these shRNAs increased their sensitivity to doxorubicin to a similar extent as with the anti-*ATM* hairpin (Fig. 3*B* and *C*). In addition, knocking down *ATR* or *Chk1* also increased the expression of the E2F target and proliferation marker *PCNA* (Fig. 3*D*). Taken together, our results suggest that the chemosensitizing effects of G_2 checkpoint inhibitors in *p53*-deficient cells are not only associated with checkpoint defects but may also involve the effects of *PCNA* and other E2F target genes.

Effect of *ATM* suppression on normal human diploid fibroblasts. To evaluate whether suppressing *ATM* specifically sensitized *p53*-deficient cells we used the normal human diploid fibroblast line IMR90. These normal cells are often used as *p53* wild-type control cells and may allow us to discern whether the effects of *ATM* small interfering RNAs and DNA-damaging agents may spare normal cells. One limitation of using primary cells is their inability to form colonies in a clonogenic assay. Therefore, we used a growth assay on the whole cell population to evaluate the effects of drugs and *ATM* inhibition in these cells.

After infection of IMR90 with the retroviral vectors expressing anti-*ATM* hairpins and ribozymes, the degree of *ATM* inhibition was similar to that obtained in PC3 cells (Fig. 4*A*). Again, the shRNA was more effective than ribozymes in reducing *ATM* gene expression. Neither the hairpins nor the ribozymes significantly inhibited cell growth in IMR90 cells (Supplementary Fig. 3*A*). Treatment with doxorubicin, at the concentration used in PC3 cells, led to inhibition of cell growth by a factor of 1.6. Notably, reducing *ATM* gene expression with RNA hairpins or ATM-Rz1 made these cells more resistant to the toxic effects of doxorubicin (Fig. 4*B*). This is consistent with a role of ATM in sensing DNA damage and activating p53-dependent cell death (22). Finally, treating IMR90 cells with doxorubicin plus UCN-01 was more effective in inhibiting cell growth, but reducing *ATM* levels with shRNA did not sensitize these cells to such treatment (Fig. 4*B*). Taken together and in contrast to the *p53*-defective PC3 cell line, normal IMR90 fibroblasts were not sensitized to DNA-damaging drugs by *ATM* knockdown.

The enhancement in chemosensitivity seen in PC3 cells but not in IMR90 cells after *ATM* inhibition could be due, at least in part, to the *p53* status of these cells or to any other of the multiple mutations present in PC3 cells and not in IMR90 cells. We reasoned that if *ATM* inhibition sensitizes *p53*-defective cells to chemotherapy, then blocking *p53* functions in IMR90 cells should sensitize these cells to chemotherapy after *ATM* knockdown. To verify this hypothesis we used a stable cell line derived from IMR90 cells expressing a dominant-negative *p53* (IMR90-dnp53; ref. 39). IMR90-dnp53 cells were resistant to cellular senescence induced by $p14^{ARF}$, a well-known *p53* activator (39) and did not induce *p21* upon expression of oncogenic *ras* (data not shown). First, we depleted

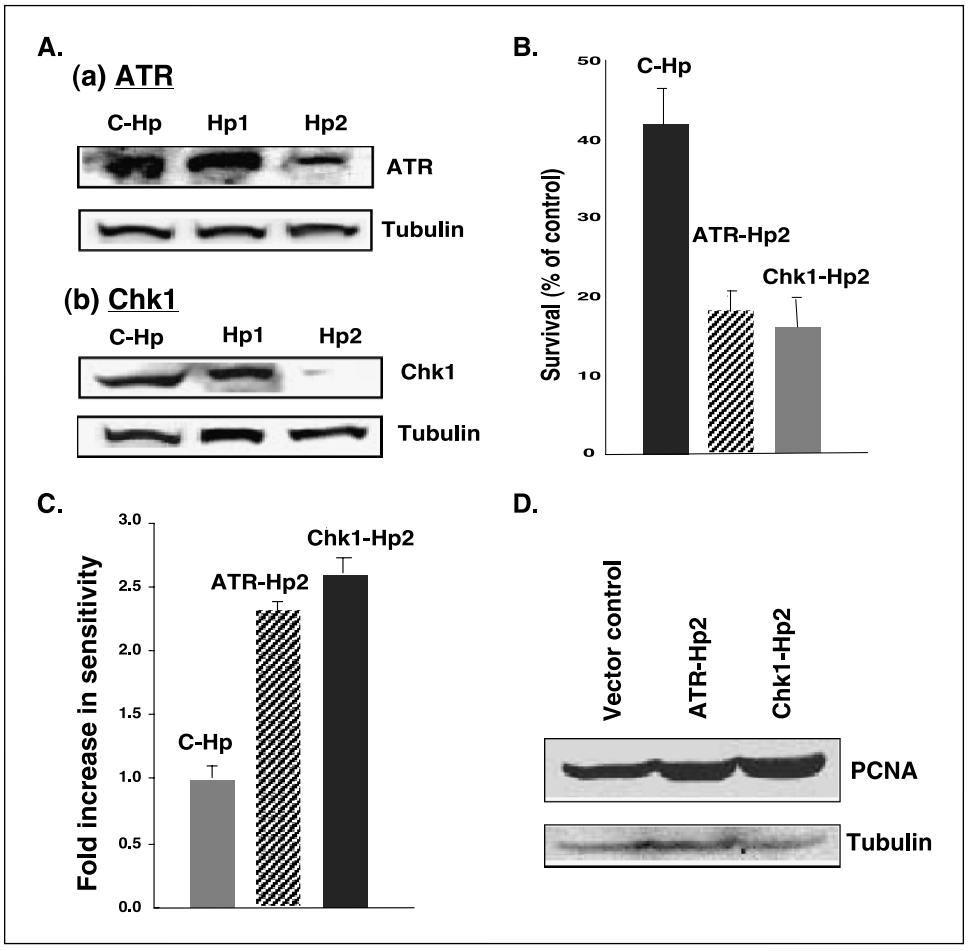

Figure 3. Enhanced chemosensitivity of ATR- or Chk1-suppressed PC3 cells. *A,* Western blot detection of ATR and Chk1 in PC3 cells with control shRNA (*C-Hp*), anti-ATR hairpin 1 (*ATR-Hp1*), anti-*ATR* hairpin 2 (*ATR-Hp2*), anti-*Chk1* hairpin 1 (*Chk1-Hp1*), and anti-Chk1 hairpin 2 (*Chk1-Hp2*). *B,* clonogenic survival assay in PC3 cells with different shRNAs after treatment with doxorubicin (20 ng/mL) or vehicle for 72 hours. *C,* sensitivity to doxorubicin for ATR- or Chk1-suppressed PC3 cells calculated from the results presented in *B* by dividing the percent survival in respective vector control with the percent survival in cells expressing anti-*ATR* or anti-*Chk1* hairpins. *D, PCNA* expression in PC3 cells expressing a vector control or shRNAs against *ATR* or *Chk1*.

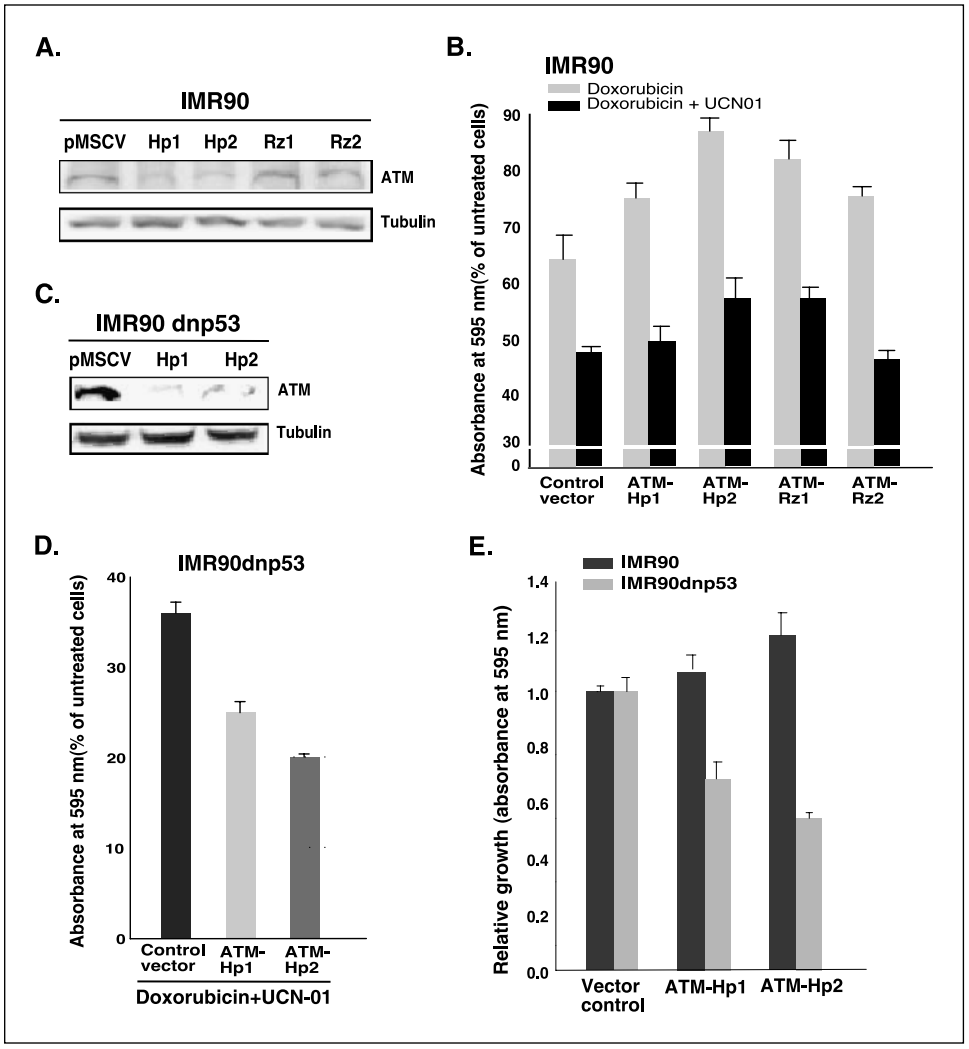

Figure 4. Effect of shRNA and hammerhead ribozyme–mediated suppression of *ATM* on normal human fibroblasts expressing a vector control or dominant-negative *p53*. *A,* Western blot detection of ATM in IMR90 cells transduced with various anti-*ATM* shRNA and ribozyme expression constructs. *B,* growth of *ATM*-suppressed IMR90 in the presence and absence of drugs. For each transduced cell line, the viability of untreated cells is taken as 100%. *C,* Western blot detection of ATM in IMR90-dnp53 cells transduced with anti-*ATM* shRNAs expressing retroviruses. *Columns,* average of three means; *bars,* SD. *D,* growth of *ATM*-suppressed, *p53*-deficient IMR90-dnp53 under treatment with drug combination (20 ng/mL doxorubicin + 100 nmol/L UCN-01). Relative absorbances compared with respective untreated controls (100%) were plotted. *E,* effects of anti-*ATM* shRNAs on the growth of IMR90 and IMR90-dnp53 in the presence of Doxorubicin + UCN-01. Values were calculated from the data presented in *B* and *D* and plotted relative to the value for respective vector control.

ATM in IMR90-dnp53 using ATM-Hp1 or ATM-Hp2 (Fig. 4*C*). *ATM* inhibition did not affect the growth of these cells (Supplementary Fig. 3*B*) but sensitized them to doxorubicin and UCN-01, as observed previously in PC3 cells (Fig. 4*D*). A comparison of the sensitivity to doxorubicin and UCN-01 of IMR90 and IMR90-dnp53 over three different experiments is presented in Fig. 4*E*. Both anti-*ATM* shRNAs increased the sensitivity of IMR90-dnp53 to doxorubicin or doxorubicin plus UCN-01, whereas they have a moderate protecting effect against doxorubicin in IMR90 cells.

Effects of *ATM* suppression on *p53*-proficient LNCaP prostate cancer cells. The experiments described above have two caveats. First, we have used different assays to measure drug response in normal IMR90 (growth curve) and PC3 tumor cell line (clonogenic assay). Second, normal fibroblasts might have a different organization of the checkpoint pathways in comparison with prostate cells. To address these concerns we used the *p53*-proficient and androgen-sensitive prostate cell line LNCaP and its derivative, wherein we introduced dominant-negative *p53* (LNCaP-dnp53). We introduced ATM-Hp2 and a control hairpin in LNCaP and LNCaP-dnp53 cells by retroviral gene transfer and observed a similar inhibition of *ATM* expression in both cell lines (Fig. 5*A*). To determine whether dominant-negative *p53* disabled the p53 pathway in LNCaP cells we tested the expression of *p21*, a known *p53* downstream protein. As expected, dnp53 decreased the basal levels of p21 in this cell line. p21 levels in doxorubicin-treated cells were also significantly inhibited by dnp53 (Fig. 5*A*, *bottom*). Interestingly, the anti-*ATM* shRNA also reduced the basal levels of p21 in LNCaP cells. This is consistent with an ATM requirement for some but not all p53 functions (40). This reduction was not observed in cells treated with doxorubicin.

Next we treated LNCaP cells and LNCaP-dnp53 cells expressing the anti-*ATM*-hairpin or a hairpin control with doxorubicin, UCN-01, or a combination of doxorubicin and UCN-01. It is worth mentioning that although 100 nmol/L UCN-01 did not significantly affect PC3 cells, it did reduce growth and clonogenicity of LNCaP cells (Supplementary Fig. 1). Regardless of this difference, *p53*-proficient LNCaP cells behaved like IMR90 cells; that is, reduction of *ATM* expression did not increase their sensitivity to the chemotherapeutic drugs used (Fig. 5*B*). In contrast, *p53*-disabled LNCaP-dnp53 cells were more sensitive to doxorubicin, UCN-01, or doxorubicin plus UCN-01 after inhibition of *ATM* expression (Fig. 5*C*; Supplementary Fig. 1). As seen in PC3 cells, anti-*ATM* shRNA increased the sensitivity of LNCaP-dnp53 by a factor of 3.4 (Fig. 5*D*) and had no effect or even brought slight protection to *p53* wild-type LNCaP (Fig. 5*D*). Cell cycle analysis in LNCaP cells showed that ATM-Hp2 moderately decreased the percentage of cells in G_2-M in untreated cells but not in cells treated with doxorubicin (Fig. 5*E*). Thus, the G_2 checkpoint in LNCaP cells is less dependent on ATM than in PC3

cells, because *ATM*-depleted PC3 cells exposed to doxorubicin showed a clear decrease in the G_2 phase. Addition of UCN-01 decreased the number of cells in G_2-M in both cells not treated and treated with doxorubicin. Because UCN-01 blocks additional G_2 checkpoint regulators (i.e., Chk1) this result is consistent with the idea that the ATR-Chk1 pathway, targeted by UCN-01, plays an important role in the control of the G_2 checkpoint in LNCaP cells.

In LNCaP-dnp53 cells, expression of the shRNA against *ATM* actually increased the number of cells arrested in G_2-M (Fig. 5*E*). Hence, blocking *p53* and *ATM* may trigger a compensatory prolongation of G_2-M in LNCaP cells. UCN-01 reduced the number of cells arrested in G_2-M after treatment with doxorubicin in LNCaP-dnp53 as well (Fig. 5*E*). The data suggest that in LNCaP-dnp53 cells, abrogation of the G_2 checkpoint cannot explain the increased sensitivity to doxorubicin after *ATM* depletion. However, abrogation of this checkpoint with UCN-01 improved the killing efficiency of doxorubicin.

We then investigated whether an increase in E2F activity was associated with *ATM* depletion in LNCaP cells. To do the experiment we did similar reporter assays as described with PC3 cells. We found that *ATM* depletion moderately increased E2F activity in LNCaP-dnp53 but not in LNCaP wild-type cells. More importantly, upon treatment with doxorubicin E2F activity significantly increased only in LNCaP-dnp53 *ATM*-depleted cells (Fig. 5*F*). Taken together, the data suggest that in LNCaP cells the chemosensitizing effects of *ATM* knockdown require a disabled *p53* and is linked to induction of E2F activity by doxorubicin.

Suppressing *ATM* gene expression in *p53* null cells increase cell death in response to DNA-damaging drugs. We have shown that reducing *ATM* levels by shRNA sensitizes PC3, LNCaP-dnp53, and IMR90-dnp53 to doxorubicin or a combination of doxorubicin and UCN-01. We have measured this effect in clonogenic survival and growth assays. These assays score growth inhibition without distinguishing cell cycle arrest from cell death. To gain further insight into the mechanisms of cell growth inhibition after treatment with doxorubicin and UCN-01 we measured cell death by a trypan blue staining assay. We found a good correlation between the percentage of cell death as

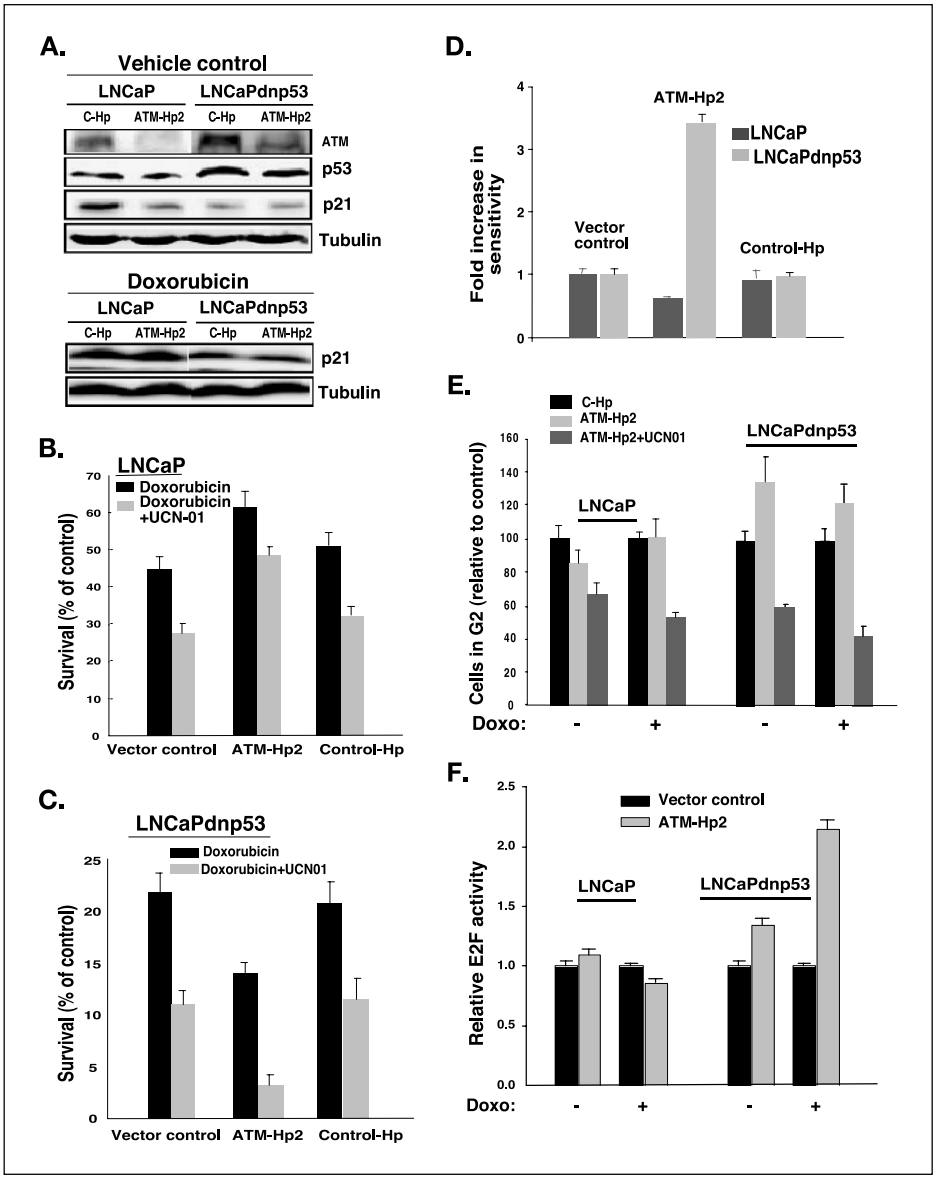

Figure 5. Chemosensitivity of LNCaP and LNCaP-dnp53 cells after knockdown of *ATM*. *A,* Western blot detection of ATM, p53, and p21 from stably transduced LNCaP and LNCaP-dnp53 treated or not treated with doxorubicin. *B* and *C,* clonogenic survival assay of LNCaP and LNCaP-dnp53 cells expressing a control vector, anti-*ATM* shRNA, or a control shRNA. Cells were treated with doxorubicin or doxorubicin + UCN-01 and survival was expressed as percentage of respective untreated controls (100%). *D,* fold increase in sensitivity to the drug mixture (i.e., doxorubicin + UCN01) for *ATM*-suppressed LNCaP and LNCaP-dnp53 cells were calculated from the results presented in *B* and *C* by dividing the percent survival in cells expressing vector control with the percent survival in cells expressing anti–ATM-Hp2. *E,* effect of shRNA against *ATM*, and a control shRNA on the relative abundance of cells in G_2-M stage of the cell cycle in cells treated or not treated with doxorubicin or UCN-01. *F, ATM* knockdown increases E2F activity only in LNCaP-dnp53 cells. LNCaP and LNCaP-dnp53 cells were cotransfected with the luciferase reporter construct HsOrc1-luc, which contains E2F sites and a vector control or its derivative expressing anti–ATM-Hp2. Cells were then treated with doxorubicin or vehicle. *Columns,* average of three means; *bars,* SD.

measured by trypan blue staining and the degree of growth inhibition reported previously. For example, drugs induced much more cell death in PC3 cells expressing an anti-*ATM* hairpin than in control PC3 cells (Fig. 6*A*). This cell death had features of apoptosis such as fragmented DNA into multimers of nucleosomal-sized (180 bp) fragments (Fig. 6*B*; ref. 30). In contrast, depletion of *ATM* in *p53*-proficient IMR90 or LNCaP cells did not lead to an increase of cell death over the value of control cells with wild-type levels of ATM. On the contrary, *ATM* knockdown protected these cells from the killing effects of the drugs (Fig. 6*C* and *D*). It is remarkable that the drug combination UCN-01 + doxorubicin killed ~15% of PC3 and around 40% of IMR90 cells after 4 days in culture. In contrast, upon *ATM* knockdown the sensitivity of PC3 cells increased whereas normal IMR90 fibroblasts became more resistant to the treatment. Taken together, our results show that PC3 cells were three times more resistant to drug treatment than normal fibroblasts (Fig. 6*A* and *C*). However, *ATM* knockdown exquisitely sensitized PC3 cells while conferring protection to normal cells. In agreement with the results presented above, the ability of the anti-*ATM* shRNA to sensitize cells to doxorubicin-induced cell death was dependent on the *p53* status. Blocking *p53* functions in IMR90 and LNCaP cells changed their response to *ATM* inhibition, making them more sensitive to drug-induced cell death (Fig. 6*C* and *D*). Therefore, *p53*-deficient cells are more sensitive to DNA-damaging agents when *ATM* is depleted. Moreover, reduction of ATM levels not only sensitized *p53* mutant tumor cells to chemotherapy but also protected normal cells from DNA-damaging agents.

Discussion

We have shown that silencing *ATM* expression with shRNAs increased the effect of chemotherapy in *p53*-deficient cells but not in *p53*-proficient cells. Because *p53* is inactivated in at least 50% of human cancers, drugs targeting ATM and, perhaps, other checkpoint regulators should be highly valuable in treating patients suffering from neoplastic diseases. Previous studies in PC3 prostate cancer cells reached a similar conclusion (23–25). However, other mutations present in those cells could be responsible for their chemosensitivity. Here we directly examined the role of *p53* status in chemosensitivity by disabling *p53* in normal human diploid fibroblasts and in the *p53*-proficient LNCaP cells by stable expression of dominant-negative *p53*. Because IMR90 cells do not posses oncogenic mutations and LNCaP cells are poorly tumorigenic their increased chemosensitivity after disabling both *p53* and *ATM* gives substantial support to the concept of selective killing of *p53*-deficient cells at any stage of tumor formation.

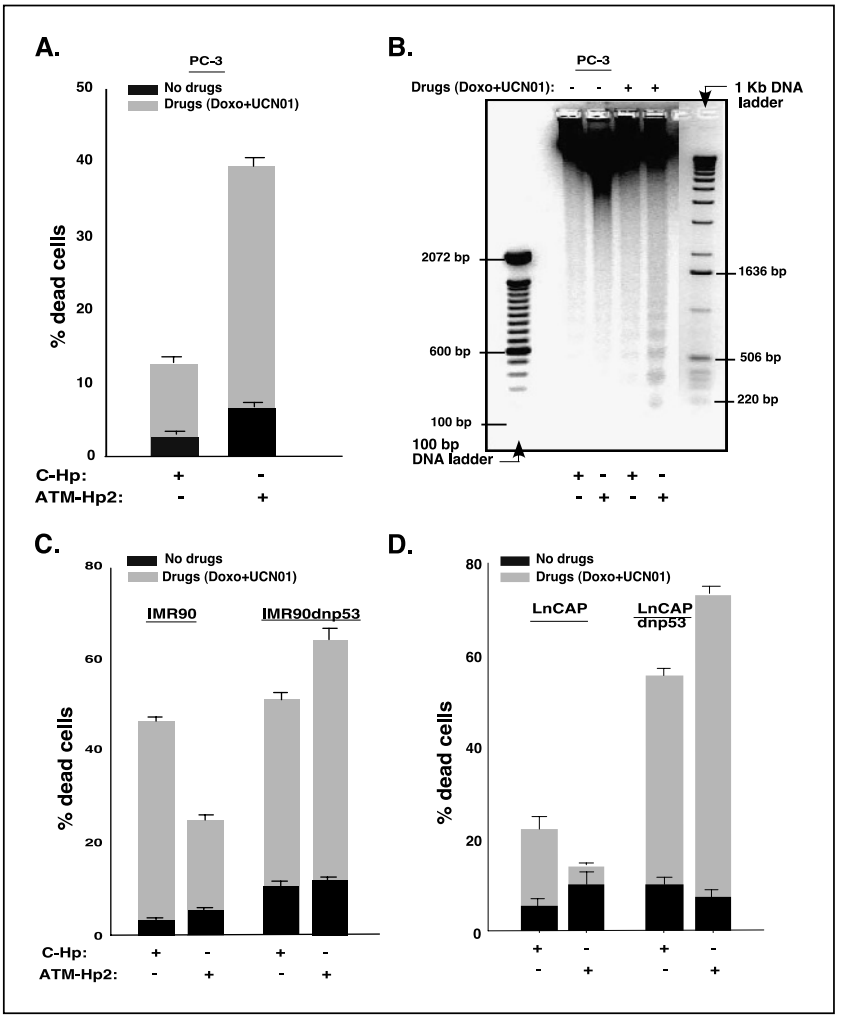

Figure 6. Cell death as a result of *ATM* deprivation in normal or prostate cancer cells with or without *p53*. *A,* cell death (Trypan blue dye exclusion) assay for PC3 cells. *B,* DNA fragmentation (DNA ladders) in PC3 cells after treatment with doxorubicin. *C,* cell death assay for *p53*-proficient/deficient IMR90. *D,* cell death assay for LNCaP and LNCaP-dnp53. For the cell death assay, we counted the percentages of blue cells in a total of 500 cells for each condition in three independent experiments. *Columns,* average of three means; *bars,* SD.

It might seem paradoxical that *p53*-deficient cells can be sensitized to DNA-damaging drugs inasmuch as p53 is a major mediator of cell death in response to DNA damage (17). We propose that different effects of *p53* and *ATM* inhibition cooperate to increase chemosensitivity (Fig. 7). We agree with previous reports that reducing ATM levels and inhibiting the S-G_2 checkpoints should be more deleterious in *p53*-deficient cells, in which the G_1 checkpoint is already compromised (22). This idea is consistent with models proposing that *p53* seems to be more prominent in the control of DNA repair and the G_1 checkpoint (19), whereas ATM is a major regulator of the S and G_2 checkpoints (41). Consistent with this explanation, the Chk1 inhibitor UCN-01 cooperated with the anti-*ATM* shRNA to increase chemosensitivity. However, our data also indicate that checkpoint inhibition is not the only mechanism explaining the chemosensitivity of cells lacking both *p53* and *ATM*. We have found that cells with defective *p53* and *ATM* possess a unique biochemical signature that may explain their increased sensitivity to DNA-damaging drugs. These molecular changes include a dramatic increase in mitotic index, augmented *PCNA* expression and E2F activity, and a poor expression of *p21*. These changes may act in separate pathways but they may also promote synergistic interactions. For example, p21 is a major PCNA inhibitor (42); thus, cells disabled for both *p53* and the ATM/ATR checkpoint pathways may have a synergistic increase in PCNA activity.

PCNA may increase drug sensitivity by accelerating DNA replication (35), inducing p53-independent apoptosis via the candidate tumor suppressor ING1b (43, 44), or promoting translesion DNA synthesis by faulty DNA polymerases (45–47). For its part, E2F activity may increase drug sensitivity by inducing proapoptotic genes such as *p73*, *Apaf1*, *caspase 3*, and *caspase 7* (36–38). Consistent with the apoptotic mechanism we detected nucleosomal-sized DNA fragments in PC3 cells expressing anti-*ATM* shRNA after treatment with doxorubicin. It remains to be investigated how *ATM* knockdown increases E2F activity in *p53*-deficient cell but not in *p53* wild-type cells. It has been reported that active Cdk2-cyclin E complexes phosphorylate E2F5, increasing its transcriptional activity and cell cycle progression (48). The activity of Cdk2-cyclin A/E complex may be higher in cells lacking *p53* and *ATM* due to the simultaneous defects in p21, a CDK inhibitor, and Chk2, which inhibits Cdc25, a CDK activator. Hence, the simultaneous inhibition of *p53* and *ATM* creates a new cellular condition of high sensitivity to DNA damage that may result from the combined effects of checkpoint deficiencies and high E2F, PCNA, and perhaps, CDK activity.

Intriguingly, blocking *ATM* expression reduced the number of cells in G_2-M in PC3 cells but not in LNCaP cells. This result suggests that compensatory mechanisms restore the G_2 checkpoint in LNCaP cells. The G_2 checkpoint is controlled by the kinases ATM and ATR that receive DNA-damage signals activating downstream effectors such as the checkpoint kinases Chk1 and Chk2 (41, 49, 50). Chk1 and Chk2 phosphorylate and inactivate the Cdc25 family of phosphatases, which are required to dephosphorylate and activate Cdk1, an enzyme essential for cell cycle passage from G_2 to M (41). Thus, in the absence of ATM the ATR/Chk1 pathway can compensate for the G_2 checkpoint defects as has been observed in fibroblasts from patients with ataxia telangiectasia (51). In this sense, LNCaP cells are similar to murine fibroblasts wherein loss of *ATM* sensitized *p53* null cells to anticancer agents without interfering with the G_2 checkpoint (52). Together, these data support our model (Fig. 7) proposing that the chemosensitizing effect of the *ATM* knockdown is not only the result of checkpoint defects.

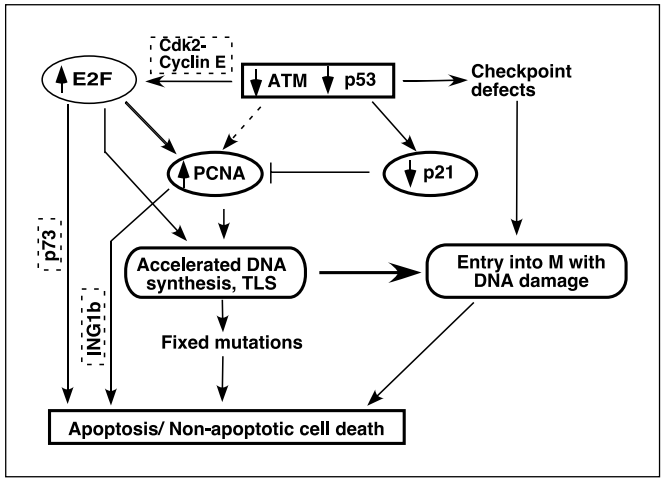

Figure 7. Model to explain the increased sensitivity to DNA damage after knocking down *ATM* in *p53* null cells. Cells without *p53* and *ATM* combine checkpoint defects with a high E2F activity and a synergistic increase in *PCNA* functions. The latter is the result of an increased *PCNA* expression due to *ATM* knockdown and a poor *p21* expression due to *p53* mutations. The mechanism of PCNA increase after *ATM* knockdown is presently unknown but it may as well involve E2F. E2F activity may increase due to high Cdk2-cyclin E activity resulting from defects in two of its inhibitory influences: (*a*) the checkpoint controlled tyrosine phosphorylations normally activated by ATM and (*b*) the CDK inhibitor *p21*, a p53 target gene. *TLS,* translesion DNA synthesis.

Because in our experiments we have disabled the ATM/Chk2 or the ATR/Chk1 pathway, a critical question is how the cells that survived the treatment handle DNA damage. As mentioned before, the ATR/Chk1pathway can compensate for ATM/Chk2 defects and vice versa (51). Microarray analysis of *p53* null and *ATM* null cells could suggest potential compensatory pathways. For example, B-cell lymphocytic leukemia cells with disabled *ATM* and *p53* express high levels of the Rad51-like protein XRCC2, a protein that mediates homologous recombination (53). Several studies point to a causal role for the homologous recombination repair pathway in resistance to DNA-damaging drugs (54). Hence, combining G_2 checkpoint blockers with inhibitors of homologous recombination might enhance the efficacy of chemotherapy (53, 55).

An additional important finding of our study is that inhibiting *ATM* functions by shRNA did not sensitize normal human fibroblasts to doxorubicin. This observation contrasts with the well-known susceptibility of *ATM* null cells to agents causing DNA-strand breaks. This difference might simply result from the short duration of our growth test (1-2 weeks) or the low concentration of doxorubicin used in our experiments. It is also possible that the low levels of ATM not inhibited by RNAi can still carry out some essential functions. This is a very important issue and a good reason to use RNAi instead of complete knockouts to validate whether a particular gene is a good target to develop drugs against cancer.

In conclusion, we have described a strategy that moderately increase the sensitivity of tumor cells to chemotherapy and at the same time protects normal cells. Because chemotherapy works on a very narrow therapeutic window, knocking down *ATM*, and perhaps other G_2 checkpoint regulators, may significantly improve current cancer therapeutics. In particular, prostate tumors, known for their low proliferation rates, are resistant to chemotherapeutic agents (56). Interfering with *ATM* functions may be a useful strategy to force slow-growing prostate tumor cells into rapidly cycling cells more susceptible to chemotherapy.

Acknowledgments

Received 7/15/2004; revised 12/5/2004; accepted 1/19/2005.

Grant support: Canadian Prostate Cancer Research Idea Initiative and the Prostate Cancer Research Foundation of Canada (G. Ferbeyre).

The costs of publication of this article were defrayed in part by the payment of page charges. This article must therefore be hereby marked *advertisement* in accordance with 18 U.S.C. Section 1734 solely to indicate this fact.

We thank Drs. Moulay Alaoui-Jamali, V. Bourdeau, and A. Mukhopadhyay and members of the Ferbeyre laboratory for reviewing the manuscript, Dr. J. De Gregory for E2F reporter construct, Dr. M. Kastan for anti-ATM antibody, and Dr. Mario Chevrette for LNCaP cells.

References

1. Hartwell LH, Weinert TA. Checkpoints: controls that ensure the order of cell cycle events. Science 1989;246: 629–34.

2. Paulovich AG, Toczyski DP, Hartwell LH. When checkpoints fail. Cell 1997;88:315–21.

3. Senderowicz AM. Small-molecule cyclin-dependent kinase modulators. Oncogene 2003;22:6609–20.

4. Heidenberg HB, Sesterhenn IA, Gaddipati JP, et al. Alteration of the tumor suppressor gene p53 in a high fraction of hormone refractory prostate cancer. J Urol 1995;154:414–21.

5. Heidenberg HB, Bauer JJ, McLeod DG, Moul JW, Srivastava S. The role of the p53 tumor suppressor gene in prostate cancer: a possible biomarker? Urology 1996; 48:971–9.

6. Harris CC, Hollstein M. Clinical implications of the p53 tumor-suppressor gene. N Engl J Med 1993;329: 1318–27.

7. Qian J, Hirasawa K, Bostwick DG, et al. Loss of p53 and c-myc overrepresentation in stage T(2-3)N(1-3)M(0) prostate cancer are potential markers for cancer progression. Mod Pathol 2002;15:35–44.

8. Verma RS, Manikal M, Conte RA, Godec CJ. Chromosomal basis of adenocarcinoma of the prostate. Cancer Invest 1999;17:441–7.

9. Leite KR, Franco MF, Srougi M, et al. Abnormal expression of MDM2 in prostate carcinoma. Mod Pathol 2001;14:428–36.

10. Downing SR, Jackson P, Russell PJ. Mutations within the tumour suppressor gene p53 are not confined to a late event in prostate cancer progression. A review of the evidence. Urol Oncol 2001;6:103–10.

11. Downing SR, Russell PJ, Jackson P. Alterations of p53 are common in early stage prostate cancer. Can J Urol 2003;10:1924–33.

12. Henke RP, Kruger E, Ayhan N, Hubner D, Hammerer P, Huland H. Immunohistochemical detection of p53 protein in human prostatic cancer. J Urol 1994;152: 1297–301.

13. Stricker HJ, Jay JK, Linden MD, Tamboli P, Amin MB. Determining prognosis of clinically localized prostate cancer by immunohistochemical detection of mutant p53. Urology 1996;47:366–9.

14. Van Veldhuizen PJ, Sadasivan R, Cherian R, Dwyer T, Stephens RL. p53 expression in incidental prostatic cancer. Am J Med Sci 1993;305:275–9.

15. Stapleton AM, Timme TL, Gousse AE, et al. Primary human prostate cancer cells harboring p53 mutations are clonally expanded in metastases. Clin Cancer Res 1997;3:1389–97.

16. Navone NM, Labate ME, Troncoso P, et al. p53 mutations in prostate cancer bone metastases suggest that selected p53 mutants in the primary site define foci with metastatic potential. J Urol 1999; 161:304–8.

17. Vogelstein B, Lane D, Levine AJ. Surfing the p53 network. Nature 2000;408:307–10.

18. Wani MA, Zhu Q, El-Mahdy M, Venkatachalam S, Wani AA. Enhanced sensitivity to anti-benzo(*a*) pyrene-diol-epoxide DNA damage correlates with decreased global genomic repair attributable to abrogated p53 function in human cells. Cancer Res 2000;60:2273–80.

19. Smith ML, Ford JM, Hollander MC, et al. p53-mediated DNA repair responses to UV radiation: studies of mouse cells lacking p53, p21, and/or gadd45 genes. Mol Cell Biol 2000;20:3705–14.

20. Bache M, Pigorsch S, Dunst J, et al. Loss of G2/M arrest correlates with radiosensitization in two human sarcoma cell lines with mutant p53. Int J Cancer 2001;96:110–7.

21. Yao SL, Akhtar AJ, McKenna KA, et al. Selective radiosensitization of p53-deficient cells by caffeine-mediated activation of p34cdc2 kinase. Nat Med 1996; 2:1140–3.

22. Shiloh Y. ATM and related protein kinases: safeguarding genome integrity. Nat Rev Cancer 2003; 3:155–68.

23. Fan Z, Chakravarty P, Alfieri A, Pandita TK, Vikram B, Guha C. Adenovirus-mediated antisense ATM gene transfer sensitizes prostate cancer cells to radiation. Cancer Gene Ther 2000;7:1307–14.

24. Guha C, Guha U, Tribius S, et al. Antisense ATM gene therapy: a strategy to increase the radiosensitivity of human tumors. Gene Ther 2000;7:852–8.

25. Collis SJ, Swartz MJ, Nelson WG, DeWeese TL. Enhanced radiation and chemotherapy-mediated cell killing of human cancer cells by small inhibitory RNA silencing of DNA repair factors. Cancer Res 2003;63: 1550–4.

26. Kawabe T. G2 checkpoint abrogators as anticancer drugs. Mol Cancer Ther 2004;3:513–9.

27. Ferbeyre G, de Stanchina E, Querido E, Baptiste N, Prives C, Lowe SW. PML is induced by oncogenic ras and promotes premature senescence. Genes Dev 2000; 14:2015–27.

28. Serrano M, Lin AW, McCurrach ME, Beach D, Lowe SW. Oncogenic ras provokes premature cell senescence associated with accumulation of p53 and p16INK4a. Cell 1997;88:593–602.

29. Paddison PJ, Hannon GJ. RNA interference: the new somatic cell genetics? Cancer Cell 2002;2:17–23.

30. Sellins KS, Cohen JJ. Cytotoxic T lymphocytes induce different types of DNA damage in target cells of different origins. J Immunol 1991;147:795–803.

31. Gillies RJ, Didier N, Denton M. Determination of cell number in monolayer cultures. Anal Biochem 1986; 159:109–13.

32. Ohtani K, DeGregori J, Leone G, Herendeen DR, Kelly TJ, Nevins JR. Expression of the HsOrc1 gene, a human ORC1 homolog, is regulated by cell proliferation via the E2F transcription factor. Mol Cell Biol 1996;16:6977–84.

33. Kawasaki H, Taira K. Identification of genes by hybrid ribozymes that couple cleavage activity with the unwinding activity of an endogenous RNA helicase. EMBO Rep 2002;3:443–50.

34. Busby EC, Leistritz DF, Abraham RT, Karnitz LM, Sarkaria JN. The radiosensitizing agent 7-hydroxystaurosporine (UCN-01) inhibits the DNA damage checkpoint kinase hChk1. Cancer Res 2000;60: 2108–12.

35. Yao N, Turner J, Kelman Z, et al. Clamp loading, unloading and intrinsic stability of the PCNA, β and gp45 sliding clamps of human, *E. coli* and T4 replicases. Genes Cells 1996;1:101–13.

36. Muller H, Bracken AP, Vernell R, et al. E2Fs regulate the expression of genes involved in differentiation, development, proliferation, and apoptosis. Genes Dev 2001;15:267–85.

37. Irwin M, Marin MC, Phillips AC, et al. Role for the p53 homologue p73 in E2F-1-induced apoptosis. Nature 2000;407:645–8.

38. Stiewe T, Putzer BM. Role of the p53-homologue p73 in E2F1-induced apoptosis. Nat Genet 2000;26:464–9.

39. Mallette FA, Goumard S, Gaumont-Leclerc MF, Moiseeva O, Ferbeyre G. Human fibroblasts require the Rb family of tumor suppressors, but not p53, for PML-induced senescence. Oncogene 2004;23:91–9.

40. Barlow C, Brown KD, Deng CX, Tagle DA, Wynshaw-Boris A. Atm selectively regulates distinct p53-dependent cell-cycle checkpoint and apoptotic pathways. Nat Genet 1997;17:453–6.

41. Matsuoka S, Huang M, Elledge SJ. Linkage of ATM to cell cycle regulation by the Chk2 protein kinase. Science 1998;282:1893–7.

42. Chen J, Jackson PK, Kirschner MW, Dutta A. Separate domains of p21 involved in the inhibition of Cdk kinase and PCNA. Nature 1995;374:386–8.

43. Scott M, Bonnefin P, Vieyra D, et al. UV-induced binding of ING1 to PCNA regulates the induction of apoptosis. J Cell Sci 2001;114:3455–62.

44. Tallen G, Riabowol K, Wolff JE. Expression of p33ING1 mRNA and chemosensitivity in brain tumor cells. Anticancer Res 2003;23:1631–5.

45. Haracska L, Johnson RE, Unk I, et al. Physical and functional interactions of human DNA polymerase η with PCNA. Mol Cell Biol 2001;21:7199–206.

46. Haracska L, Johnson RE, Unk I, et al. Targeting of human DNA polymerase iota to the replication machinery via interaction with PCNA. Proc Natl Acad Sci U S A 2001;98:14256–61.

47. Haracska L, Unk I, Johnson RE, et al. Stimulation of DNA synthesis activity of human DNA polymerase κ by PCNA. Mol Cell Biol 2002;22:784–91.

48. Morris L, Allen KE, La Thangue NB. Regulation of E2F transcription by cyclin E-Cdk2 kinase mediated through p300/CBP co-activators. Nat Cell Biol 2000; 2:232–9.

49. Liu Q, Guntuku S, Cui XS, et al. Chk1 is an essential kinase that is regulated by Atr and required for the G(2)/M DNA damage checkpoint. Genes Dev 2000;14: 1448–59.

50. Zhao H, Watkins JL, Piwnica-Worms H. Disruption of the checkpoint kinase 1/cell division cycle 25A pathway abrogates ionizing radiation-induced S and G2 checkpoints. Proc Natl Acad Sci U S A 2002;99: 14795–800.

51. Wang X, Khadpe J, Hu B, Iliakis G, Wang Y. An overactivated ATR/CHK1 pathway is responsible for the prolonged G2 accumulation in irradiated AT cells. J Biol Chem 2003;278:30869–74.

52. Fedier A, Schlamminger M, Schwarz VA, Haller U, Howell SB, Fink D. Loss of atm sensitises p53-deficient cells to topoisomerase poisons and antimetabolites. Ann Oncol 2003;14:938–45.

53. Stankovic T, Hubank M, Cronin D, et al. Microarray analysis reveals that TP53- and ATM-mutant B-CLLs share a defect in activating proapoptotic responses after DNA damage but are distinguished by major differences in activating prosurvival responses. Blood 2004;103:291–300.

54. Wang ZM, Chen ZP, Xu ZY, et al. *In vitro* evidence for homologous recombinational repair in resistance to melphalan. J Natl Cancer Inst 2001;93:1473–8.

55. Fojo T. Cancer, DNA repair mechanisms, and resistance to chemotherapy. J Natl Cancer Inst 2001; 93:1434–6.

56. Isaacs JT. The biology of hormone refractory prostate cancer. Why does it develop? Urol Clin North Am 1999;26:263–73.